LBL-41607

HIGHER-ORDER DIFFERENCING FOR FRONT PROPAGATION IN GEOTHERMAL SYSTEMS

Curtis M. Oldenburg and Karsten Pruess

Earth Sciences Division
Berkeley Lab
Berkeley, CA, 94720

ABSTRACT

We have implemented higher-order differencing total variation diminishing (TVD) schemes into the reservoir simulator TOUGH2 to reduce numerical dispersion in concentration and phase front propagation problems. Much of the existing work in the literature on higher-order differencing schemes has focused on one-dimensional tracer transport using explicit formulations for the convection-dispersion equation. We find that higher-order differencing schemes can also increase the accuracy of component transport, phase transport, and thermal energy transport in strongly advective situations in two-dimensional problems using an implicit and multicomponent framework such as TOUGH2. We apply the Leonard TVD scheme to two geothermal reservoir engineering problems involving tracer transport and phase change. The first problem considers the two-dimensional transport of tracer in a reservoir under re-injection. In the second problem, we focus on the non-isothermal phase change occurring in a one-dimensional analog of a reservoir under re-injection. In both cases, the TVD scheme proves robust and useful for reducing numerical dispersion.

INTRODUCTION

The numerical simulation of the advection of phase and concentration fronts by finite difference methods in strongly advective flow systems is affected by numerical dispersion which tends to artificially smooth sharp fronts. This problem is especially relevant to geothermal reservoir engineering problems where strong advective flow of two-phase fluids occurs through fractures during fluid production and re-injection. Numerical dispersion can be diminished by decreasing grid size, but this can greatly increase execution times and computer memory requirements. Another approach for reducing numerical dispersion is to use higher-order differencing schemes instead of single-point upstream weighting.

In higher-order differencing schemes, two upstream gridblocks are used to approximate quantities such as phase saturation (or relative permeability), species concentration, and temperature at interfaces between gridblocks. In strongly advective problems and depending on the weighting scheme used, higher-order differencing can result in oscillatory and non-physical values near sharp fronts. These well-known problems have led to the development of total variation diminishing (TVD) higher-order schemes (e.g., Sweby, 1984). TVD refers to the overall variation of quantities in the system tending to diminish with time rather than increase.

In this paper, we present the theory of TVD schemes and their implementation in TOUGH2 (Pruess, 1987; Pruess, 1991) for two-dimensional regular grids, and we show results from two example applications of geothermal re-injection problems.

MATHEMATICAL DEVELOPMENT

Finite difference methods require an accurate approximation of interface quantities for calculating the fluxes between gridblocks. Below, we briefly review the development of higher-order differencing schemes for the propagation of phase and concentration fronts. We use the symbol S as the advected quantity, but we emphasize that in all of the development below S can stand for concentration, temperature, or relative permeability in addition to saturation. The mathematical development refers to the three gridblocks shown in Fig. 1 where the flow is from left to right as shown by the large arrow. We use fully implicit time-stepping with all quantities taken at the most recent iterative step.

We begin by writing a linear approximation for S at the $i+1/2$ interface as

$$S_{i+1/2} \approx S_i + D1\left(\frac{S_{i+1} - S_i}{D1 + D2}\right) \qquad (1)$$

which can be rearranged to

$$S_{i+1/2} \approx S_i + \frac{D1}{D1 + D2}\left(S_{i+1} - S_i\right) \qquad (2).$$

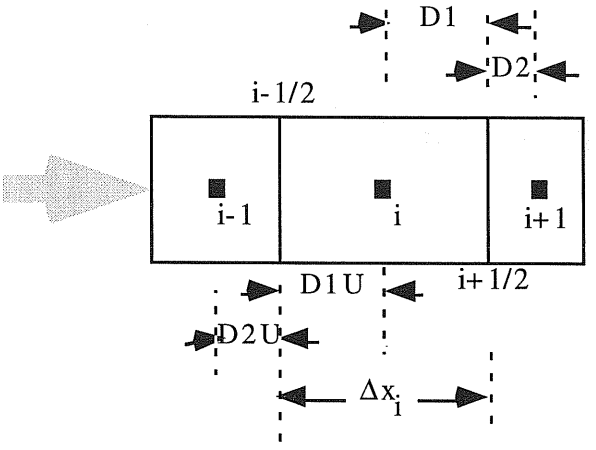

Fig. 1. Three non-uniform grid blocks with flow from left to right. The standard TOUGH2 connection is between i and i+1 and has connection distances $D1$ and $D2$ and an interface at i+1/2. Higher-order schemes use the upstream gridblock i-1 with connection distances $D1U$ and $D2U$ and the interface i-1/2.

Defining r, the ratio of upstream to downstream gradients, as follows,

$$r \equiv \frac{\left(\frac{\partial S}{\partial x}\right)_{i-1/2}}{\left(\frac{\partial S}{\partial x}\right)_{i+1/2}} = \left(\frac{S_i - S_{i-1}}{\frac{D1U + D2U}{2}} \Big/ \frac{S_{i+1} - S_i}{D1 + D2} \right) \qquad (3)$$

and rearranging to

$$r \equiv \frac{D1 + D2}{D1U + D2U} \left(\frac{S_i - S_{i-1}}{S_{i+1} - S_i} \right) \qquad (4),$$

we can propose that

$$S_{i+1/2} \approx S_i + \frac{D1}{D1 + D2} \phi(r)\left(S_{i+1} - S_i\right) \qquad (5).$$

Depending on the function $\Phi(r)$, different approximations for the interface quantity $S_{i+1/2}$ can be made (see Table 1). For example, if $\Phi(r) = 0$, the interface quantity is upstream weighted. If $\Phi(r) = 1$, a weighted average scheme results. For general $\Phi(r)$, limits (flux limiters) are imposed to make the scheme TVD. For the interface weighting scheme to be TVD, $\Phi(r)$ must fall on the heavy lines or within the shaded regions show in Fig. 2 (e.g., Sweby, 1984; Datta-Gupta *et al.*, 1991; Blunt and Rubin, 1992).

Table 1. Higher-order differencing schemes.

$\Phi(r)$	interface approximation
0	full upstream weighting
1	weighted average
r	two-point upstream
$\frac{(r + \lvert r \rvert)}{(1 + r)}$	Van Leer scheme
$2/3 + r/3$	Leonard scheme

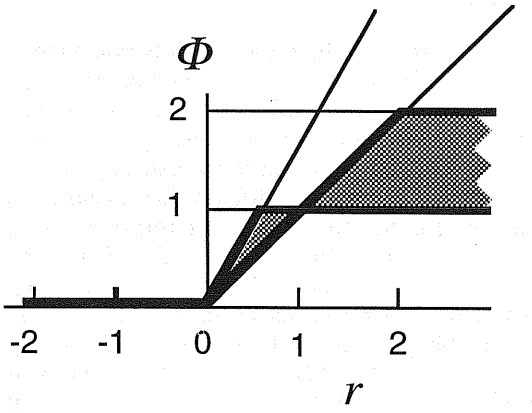

Fig. 2. The heavy lines and shaded regions show the stable values of $\Phi(r)$.

The flux limiter is applied to ensure a decrease in the total variation (TV) of the advected quantity defined as

$$TV(S)^{n+1} \equiv \sum_i \left| S_{i+1}^{n+1} - S_i^{n+1} \right| \qquad (6)$$

where n denotes the time level and the sum runs over all gridblocks i. Thus, as Eq. 6 shows, for a typical front propagation problem, the total variation will increase whenever there are jumps or oscillations in the advected quantity, S. We emphasize again that all of the development above can just as well be written for concentration, temperature, or relative permeability and equivalent weighting schemes derived for many flow situations.

We implemented higher-order differencing schemes in TOUGH2 with the restriction that the grids must be either one or two-dimensional with rectangular gridblocks. Within a TOUGH2 simulation, using higher-order TVD schemes entails finding the two upstream gridblocks, assuming locally one-dimensional flow, calculating $\Phi(r)$, applying the limiters to ensure $\Phi(r)$ is in a stable region of Fig. 2, and approximating interface values of phase saturation, relative permeability, concentration, or temperature accordingly. The Leonard scheme (LTVD) where $\Phi(r) = 2/3 + r/3$ subject to the limiters shown in Fig. 2 has proven robust and accurate (Leonard,

1984; Datta-Gupta *et al.*, 1991; Oldenburg and Pruess, 1997; Oldenburg and Pruess, 1998) and will be applied further in the remainder of this paper.

EXAMPLE APPLICATIONS

Tracer Injection

Here we compare upstream weighting and the LTVD scheme in TOUGH2/EOS7R for a test case involving injection and production from a two-dimensional sub-horizontal fracture zone. Problem specifications are similar to a production/injection problem previously studied by Pruess (1983) and Pruess and Wu (1993). Shown in Fig. 3 are the production and injection wells arranged in a five-spot pattern with 400 m well spacing. Cold water (T ≈ 30 °C) is injected at a rate of 16 kg/s (full-well basis), and production occurs at the same rate. Four kg of tracer is injected over a period of 10 days starting at $t = 0$. We model one quarter of the five-spot pattern, which was discretized into 400 square grid blocks (20 x 20) of length 10 m on a side.

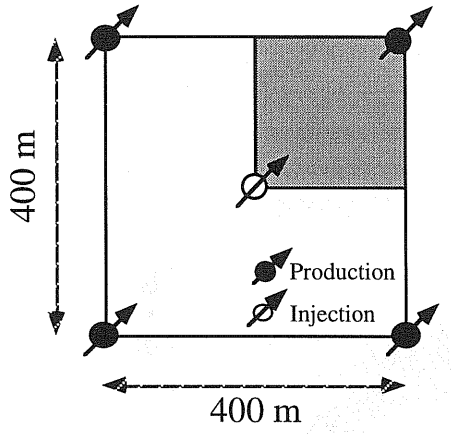

Fig. 3. Five-spot well pattern, with shading showing a 1/4 symmetry element.

The reservoir rock adjacent to the fracture zone is assumed impermeable, and at a uniform initial temperature of 300 °C. Conductive heat transfer to the fracture is modeled with the semi-analytical technique of Vinsome and Westerveld (1980). Boiling occurs near the production well as pressure declines, while cooling occurs near the injection well due to the injection of cold water. We use the module EOS7R (Oldenburg and Pruess, 1995) for components water, brine, tracer1, tracer2, air, and heat. For this preliminary application, the tracer is the brine component which is non-sorbing, non-decaying, and non-volatilizing although EOS7R is capable of handling all of these processes for the tracer1 and tracer2 components. Complete parameters for the problem are presented in Oldenburg and Pruess, 1997.

Results after 6 months computed using upstream weighting for phase saturations, component mass fractions, and thermal energy are shown in Fig. 4. The temperature field shows the effects of cold injection fluid entering the system but being retarded by conductive heating from the reservoir rocks. The tracer mass fraction field is advanced relative to heat since no retarding effects (e.g., adsorption) are present for the tracer. The saturation field shows the development of a two-phase region due to lower pressure at the production well. The final plot gives breakthrough curves of temperature and tracer mass fraction at the production well. Initial tracer breakthrough occurs at about 6 months ($t \approx 1.6 \times 10^7$ s). The retardation of the thermal front is largely masked by cooling due to boiling at the production well. In the absence of induced boiling, thermal breakthrough would be retarded by a factor of

$$R = \frac{\phi\, \rho_w\, c_w}{\phi\, \rho_w\, c_w + (1 - \phi)\, \rho_R\, c_R} \approx .55 \qquad (7)$$

where $\rho_w = 800$ kg m^{-3} and $c_w = 4000$ J kg^{-1} °C^{-1}. Note the broad region of tracer in the mass fraction plot and the gentle rise and decline of the tracer mass fraction in the breakthrough curve; these smoothing effects are due mostly to numerical dispersion.

Results after 6 months computed using the LTVD scheme for phase saturations, component mass fractions, and thermal energy are presented in Fig. 5. Comparing Figs. 4 and 5 we see generally similar results; however, note the relatively sharper fronts for temperature and especially tracer mass fraction. The phase saturation front has evolved differently using LTVD and is not as far advanced (see next application for discussion). The breakthrough curves highlight the differences in the schemes. Note the higher maximum and steeper limbs of the tracer breakthrough. Tracer would first be detected at significant concentrations after about 9 months. This sharper tracer breakthrough curve would allow a more accurate prediction of the arrival of the thermal front than the result computed using upstream weighting.

The adaptive time-stepping scheme in TOUGH2 is apparent from the symbol spacing in the breakthrough curves in Figs. 4 and 5 which show that more time steps are needed when using the higher-order scheme. Shorter time steps arise in this problem for two reasons: (1) the sharper front produces larger primary variable changes in grid blocks near the front; and (2) we did not include the dependence of the upstream grid block into the Jacobian matrix for the Newton-Raphson iteration. Because the Jacobian is less accurate, the convergence rate is reduced and the time-step size remains smaller than it would for a more accurate Jacobian matrix.

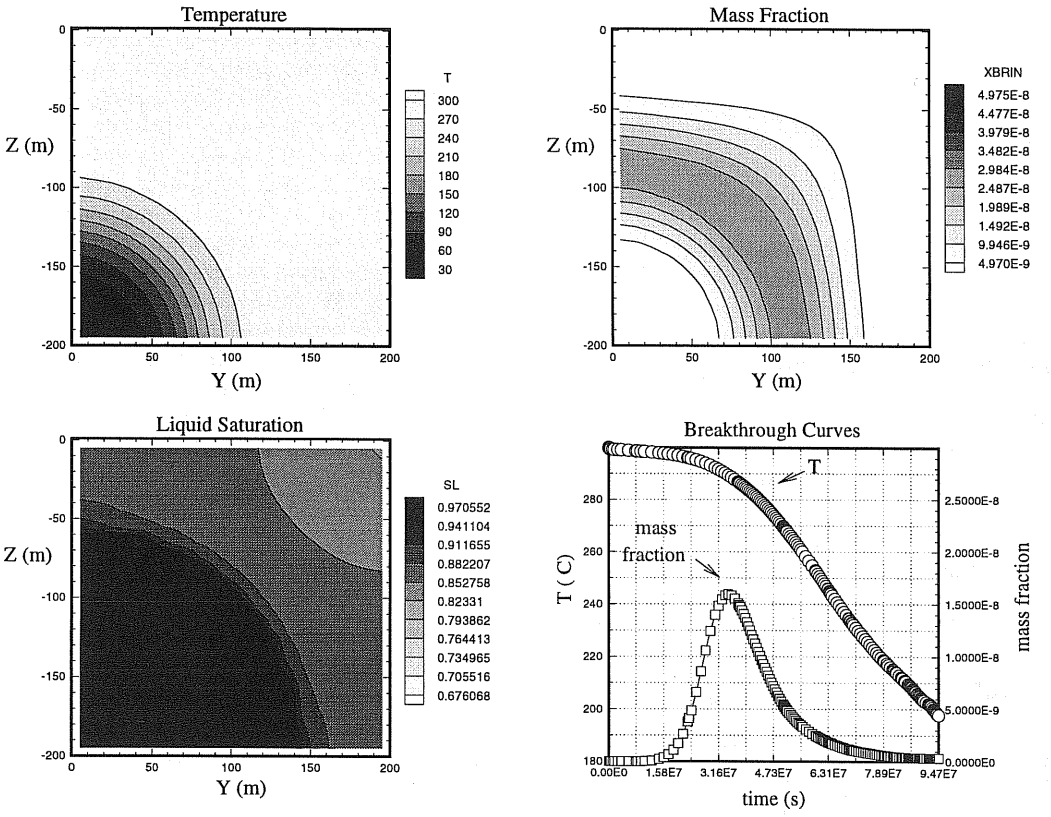

Fig. 4. Results at six months calculated using upstream weighting for two-dimensional geothermal re-injection.

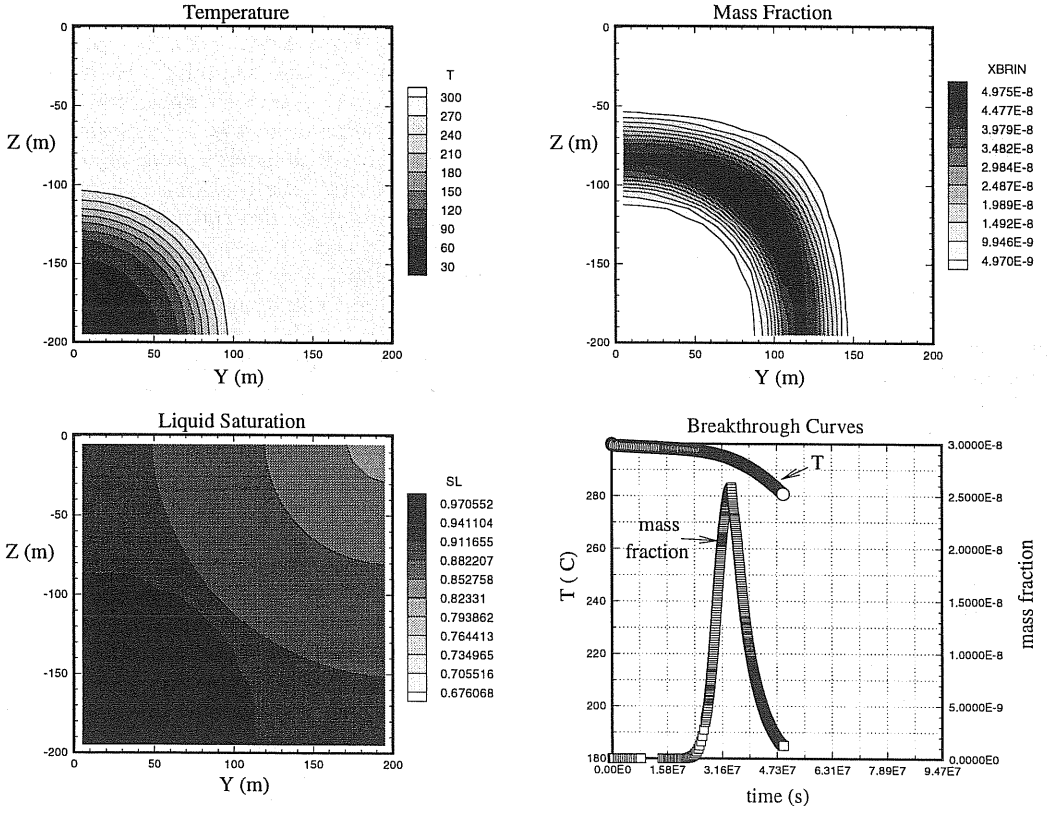

Fig. 5. Results at six months calculated using the LTVD scheme for geothermal re-injection. The run was stopped after the tail of the tracer pulse was detected.

Boiling Front

In this problem, cold (T = 30°C) water is injected into a 200 m long one-dimensional domain. The system is initially nearly single-phase liquid at the saturated vapor pressure (P_0 = 85.93 bar) at T_0 = 300 °C. A schematic of the system and initial and boundary conditions are shown in Fig. 6. Capillarity is neglected, and relative permeability is given by Corey curves. Complete parameters for the problem are presented in Oldenburg and Pruess, 1998.

The evolution begins by injecting cold water at the left-hand side at a rate of 0.4 kg/s and producing mass at the same rate from the right-hand side. The production at the right-hand side lowers the pressure and induces boiling while the cold injection water tends to produce single-phase liquid conditions. The boiling at the right-hand side causes the liquid saturations to decline from the initial conditions. Thus the difference in liquid phase saturation across the moving front increases with time making this problem physically not TVD.

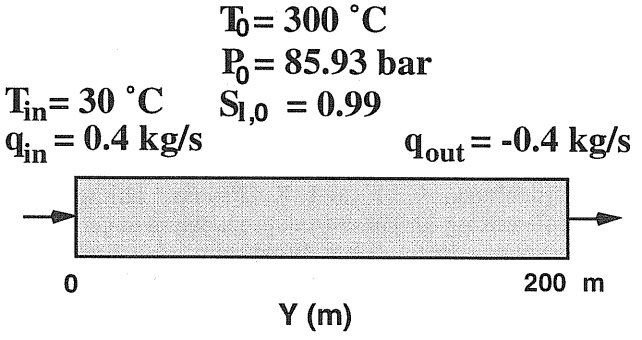

Fig. 6. Boundary and initial conditions for the one-dimensional injection and production problem.

Profiles of liquid saturation and temperature for upstream weighting and LTVD differencing schemes with 100 gridblocks are shown in Figs. 7 and 8, respectively. The temperature profiles are shown by the dashed curves while the saturation is given by the solid curves; the temperature and saturation curves intersect in the figures at the phase front. Note in Figs. 7 and 8 that the upstream-weighted results give a phase front that is farther advanced relative to the LTVD result.

Unlike typical phase displacement problems which show minimal differences whether computed by upstream weighting or by higher-order schemes, the phase front locations in this problem are significantly different in the upstream and LTVD cases. The advancement of the upstream weighted phase front relative to the LTVD phase front occurs because upstream weighting produces greater smearing of the

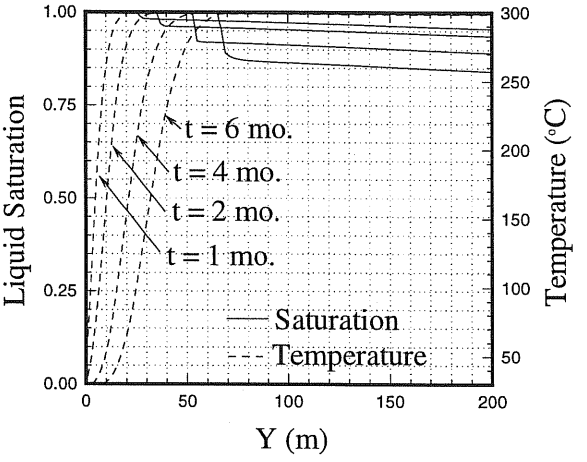

Fig. 7. Liquid saturation and temperature for the geothermal injection and production problem with upstream weighting.

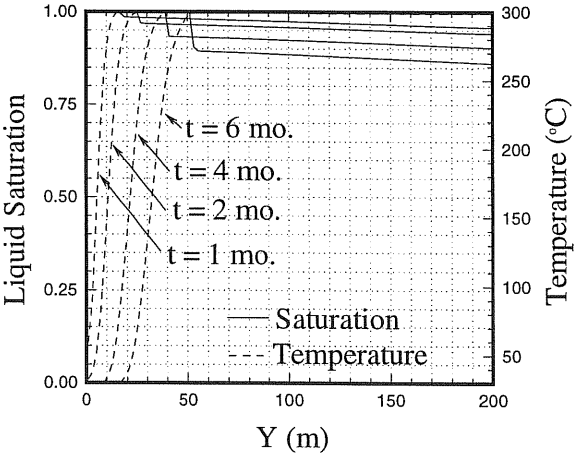

Fig. 8. Liquid saturation and temperature for the geothermal injection and production problem with LTVD scheme.

temperature front, so that saturation temperature at prevailing pressures is reached at somewhat larger distance from the injection point. The phase transition to two-phase conditions then also occurs at larger distance. In addition to the upstream and TVD-weighted simulations shown in Figs. 7 and 8, a third simulation not shown here was performed in which TVD-weighting was applied only to interface temperatures, while phase saturations were upstream-weighted. This produced results very close to those of Fig. 8, confirming that it is the numerical

dispersion of the temperature front, not that of the phase front, which causes the upstream-weighted results in Fig. 7 to deviate from the more accurate LTVD results of Fig. 8. This same phenomenon was seen in the two-dimensional example shown in the previous section.

The differences between the uptream and LTVD schemes diminish with increased resolution. We show in Fig. 9 a summary of the results of phase front location vs. number of gridblocks at a time of 6 months for this one-dimensional injection and production problem. Note in Fig. 9 that the two schemes are converging slowly but that the LTVD scheme was closer to the grid-converged result at much coarser resolution. When upstream weighting is used, numerical dispersion is proportional to ΔY (the grid spacing), and therefore diminshes slowly when grids are refined. Note finally that the fact that the saturation variation increases with time (i.e., was not TVD) posed no problem for the LTVD scheme.

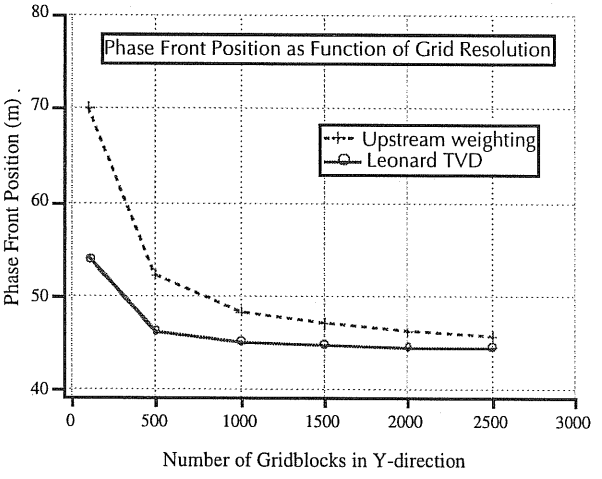

Fig. 9. Phase front location vs. grid resolution for upstream weighting and LTVD schemes at $t = 6$ months.

CONCLUSIONS

The LTVD scheme significantly reduces numerical dispersion of fronts relative to upstream weighting. The LTVD scheme has performed well on a variety of complicated problems relevant to geothermal reservoir engineering. We anticipate making available a choice of higher-order total-variation diminishing schemes in future releases of TOUGH2.

ACKNOWLEDGMENT

We thank Jens Birkhölzer and Tianfu Xu for reviews. This work was supported by the Assistant Secretary for Energy Efficiency and Renewable Energy, Geothermal Division, U.S. Department of Energy, under contract No. DE-AC03-76SF00098.

REFERENCES

Blunt, M., and B. Rubin, Implicit flux limiting schemes for petroleum reservoir simulation, *J. Comput. Physics*, *102*, 194–210, 1992.

Datta-Gupta, A., L.W. Lake, G. A. Pope, and K. Sepehnoori, High-resolution monotonic schemes for reservoir fluid flow simulation, *In Situ*, *15*(3), 289–317, 1991.

Leonard, B.P., Third-order upwinding as a rational basis for compuational fluid dynamics, in *Computational Techniques and Applications*, Elsevier Science Publishers, North-Holland, 1984.

Oldenburg, C.M. and K. Pruess, EOS7R: radionuclide transport for TOUGH2, Lawrence Berkeley Ntaional Laboratory Report *LBL-34868*, November, 1995.

Oldenburg, C.M. and K. Pruess, Mixing with first-order decay in variable-velocity porous media flow, *Transport in Porous Media*, *22*, 161–180, 1996.

Oldenburg, C.M. and K. Pruess, Higher-order differencing for geothermal reservoir simulation, Proc. 22nd Workshop on Geothermal Reservoir Engineering, Stanford University, Stanford CA, January 27–29, 1997. SGP-TR-155

Oldenburg, C.M. and K. Pruess, Higher-order differencing for phase-front propagation in geothermal systems, Proc. 23rd Workshop on Geothermal Reservoir Engineering, Stanford University, Stanford CA, January 26–28, 1998. SGP-TR-158.

Pruess, K., TOUGH User's Guide, *Nuclear Regulatory Commission, Report NUREG/CR-4645*, June 1987 (also *Lawrence Berkeley Laboratory Report, LBL-20700*, June 1987).

Pruess, K., TOUGH2- A general-purpose numerical simulator for multiphase fluid and heat flow, *Lawrence Berkeley National Laboratory Report LBL-29400*, May 1991.

Pruess, K., and Y.-S. Wu, A new semi-analytical method for numerical simulation of fluid and heat flow in fractured reservoirs, *SPE Advanced Technology Series*, *1*(2), 63–72, 1993.

Sweby, P.K., High resolution schemes using flux limiters for hyperbolic conservation laws, *SIAM J. Numer. Anal.*, *21*(5), 995–1011, 1984.

Vinsome, P. K. W. and J. Westerveld. A Simple Method for Predicting Cap and Base Rock Heat Losses in Thermal Reservoir Simulators, *J. Canadian Pet. Tech.*, 19 (3), 87–90, July-September 1980.